HELIOSEISMIC CONSTRAINTS ON THE PROPERTIES OF THE SOLAR CORE AND ON THE SOLAR NEUTRINO FLUXES

A.G. Kosovichev
W.W.Hansen Experimental Physics Laboratory
and Stanford-Lockheed Institute for Astrophysical and Space Research
Stanford University, Stanford, CA94305-4085, U.S.A.

Abstract

The temperature and the abundance of hydrogen in the Sun's interior are estimated by the method of 'secondary' inversion of solar oscillation frequencies. In this method, the equations of state and thermal balance are used in addition to the hydrostatic equations. The temperature of the solar core estimated from the current helioseismic data is slightly higher than in the standard solar model, that favors the MSW solution of the solar neutrino problem. We discuss the technique and the uncertainties of the helioseismic estimates.

1 Introduction

The discrepancy between the results of the solar neutrino experiments and prediction of the standard solar model has provided important evidence of neutrino flavor transformation [1]. It has been shown that the uncertainties and *ad hoc* assumptions involved in solar modeling are unlikely to explain this discrepancy. Modifications of the standard solar model are significantly constrained by helioseismology which has provided robust estimates of some important properties of the Sun such as the depth of the convective zone (e.g. [2,3]), the sound-speed profile (e.g. [4,5]) and the helium abundance [6]. These inferences are used as indirect constraints on solar modeling which has achieved a great deal of sophistication. As demonstrated by J. Guzik and S. Vauclair at this meeting, element diffusion and turbulent mixing are among the most important processes determining the constitution and the structure of the Sun. The physics of these processes is complicated and currently poorly understood making the theoretical estimates of the properties of the solar structure and neutrino fluxes uncertain. Perhaps, this uncertainty cannot change the conclusion about the nature of the solar neutrino problem [1], but it may significantly affect a detailed interpretation of the neutrino experiments in terms of various versions of the Grant Unified Theory. Therefore, it is important to find approaches to determine the solar properties more precisely.

Helioseismic inversion of solar oscillation frequencies is a unique tool for directly estimating the properties of the Sun's interior. The frequencies of several thousand acoustic modes of the oscillations in the 5-min range have been measured. Unfortunately, the acoustic modes that propagate through the energy-generating central core are only weakly sensitive to the core's structure. However, the frequencies of these modes have been measured to a very high precision, with typical uncertainty of several parts in a million making them useful for constraining the core structure. The SOHO space mission [7] and the GONG network [8] which are currently under way will provide even more precise frequencies of the p modes, and, possibly, will also measure modes of lower frequency, which are more sensitive to the structure of the core.

The most important properties for estimating the fluxes of neutrino are the element abundances and the temperature near the solar center. There are two basic ways of obtaining the information. The first calibrates theoretical solar models by comparing either the observed oscillation frequencies with the eigenfrequencies of the models, or the primary seismic parameters (e.g. the sound speed, the density and the adiabatic exponent) inverted from the observed frequencies with the corresponding parameters of the solar models.

The second approach measures abundances by direct ('secondary') inversions of the frequencies, incorporating additional equations of the stellar structure into the helioseismic inverse problem. The additional equation for estimating the composition of the convection zone is the equation of state which relates variations of the adiabatic exponent in the zones of ionization of elements to their abundances. In the radiative interior where the most abundant elements are almost totally ionized, the energy equations together with equations of the energy generation rate and the opacity are used to relate primary seismic parameters with abundances. The temperature can be estimated from the sound speed and the composition through the equation of state.

Both these approaches rely upon the usage of the nuclear reaction rates and the opacity of the solar plasma, imprecise knowledge of which may affect the helioseismic inferences. In principle, it is possible to include the uncertainty of these microscopic properties in the helioseismic inversion procedure. However, it is not clear whether this uncertainty can be disentangled from the variations of the chemical composition caused by turbulent diffusion and mixing. It could well be that the uncertainties in the microscopic physics and in turbulent diffusion and mixing mask each other. If this is the case then more vigorous constraints will have to be incorporated in the analysis.

In this paper, we neglect the uncertainties in the microscopic physics, and demonstrate how the central composition, temperature and the neutrino fluxes can be estimated by helioseismic inversion.

2 Inversion method

2.1 Helioseismic equations

For the frequency inversions, the linearized integral equations relating frequency perturbations, $\delta\nu_i$, to variations of the solar structure are derived from a variational principle. They are transformed to depend on a chosen pair of deviation variables $\boldsymbol{f}$ (e.g. $\boldsymbol{f}= (\delta \ln \rho, \delta \ln \gamma)$, where ρ is density and γ is the adiabatic exponent that are assumed to be functions of the radius, r, alone (e.g. [9]), yielding

$$\frac{\delta\nu_i}{\nu_i} = \int_0^{\mathrm{R}} \boldsymbol{K}_{\boldsymbol{f}}^{(i)} \cdot \boldsymbol{f} \,\mathrm{d}r + \frac{F(\nu_i)}{E_l(\nu_i)}, \quad i = 1, ..., N. \tag{1}$$

Here $\delta\nu_i$ is the frequency difference between the eigenfrequency ν_i of a solar model and the corresponding frequency of the Sun, R is the radius of the Sun, and $E_l(\nu_i)$ is the mode inertia. The arbitrary function $F(\nu_i)$ is added to take into account surface effects. The subscript i labels the modes; N is the total number of modes in a data set.

The structure parameters $\boldsymbol{f}$ can be of two types: 'primary', e.g. the density, ρ, and the sound speed, c, or 'secondary', e.g. the abundances of hydrogen, X, and heavy elements, Z. For the 'primary' parameters Eq. (1) is derived under the basic assumptions about the solar structure: spherical symmetry and hydrostatic equilibrium; whereas for the 'secondary' parameters additional structure equations must be considered. Only two structure variables appear in Eq. (1) because in deriving them the equations of hydrostatic support

$$\frac{dp}{dr} = -\frac{Gm\rho}{r^2}; \qquad \frac{dm}{dr} = 4\pi\rho r^2 \tag{2}$$

have been imposed.

We have studied two main options for the 'secondary' parameters. The first [6] includes the equation of state in the form $\gamma = \gamma(p, \rho, X_j)$, where X_j are element abundances. Since the variations of the adiabatic exponent, γ, occur mainly in the zones of ionization of helium and hydrogen at the top of the convection zone, the frequency variations can be expressed in terms of the uniform helium abundance in the convection zone (assuming that the abundances of the heavier elements are known) and one of the hydrostatic variable, e.g. density or the ratio $u = p/\rho$.

The second option [10] is to consider a full set of structure equations, including the equations of thermal balance and of energy transport, thus introducing 'non-seismic' variables, such as temperature, elemental abundance and opacities in the radiative zone, into the seismic equations.

Equations (1) can be transformed into a relation between $\frac{\delta\nu_i}{\nu_i}$ and composition deviations δX and δZ by additionally imposing the constraint of thermal balance through the equations

$$\frac{dL}{dr} = 4\pi\rho r^2\epsilon, \tag{3}$$

$$\frac{dT}{dr} = \begin{cases} -\dfrac{3\kappa\rho L}{64\pi\sigma r^2 T^3} & \text{in radiative zones} \\[2ex] \left(\dfrac{dT}{dr}\right)_c & \text{in the convection zone} \end{cases} \tag{4}$$

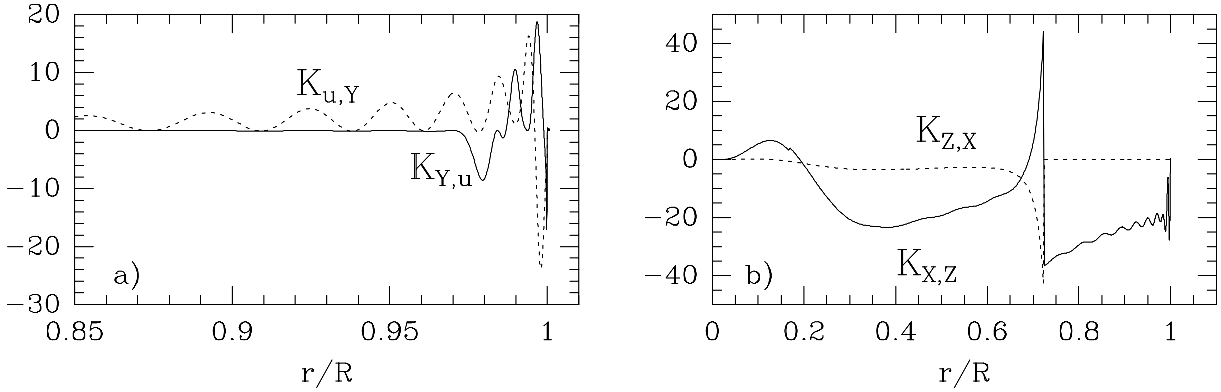

Figure 1: Seismic kernels of the p mode of the angular degree $l = 2$ and the radial order $n = 16$: a) for the parameter $u = p/\rho$ (solid curve) and for the helium abundance Y (dashed curve); b) for the hydrogen abundance, X, (solid curve) and for the heavy element abundance, Z (dashed curve).

where L is luminosity, T is temperature, ϵ is the energy-generation rate per unit mass, κ is opacity and σ is the Stefan-Boltzmann constant. The function $(dT/dr)_c$ is provided by the mixing-length formalism relating temperature gradient to energy transport in the convection zone. In addition, the functions of $\epsilon(\rho, T, X, Z)$ and $\kappa(\rho, T, X, Z)$ and their partial derivatives are required. The transformation then yields new perturbation relations which may be written

$$\frac{\delta\nu_i}{\nu_i} = \int_0^{\mathrm{R}} \boldsymbol{K}_{\boldsymbol{g}}^{(i)} \cdot \boldsymbol{g}\,\mathrm{d}r + \frac{F(\nu_i)}{E_l(\nu_i)}, \quad i = 1, ..., N \tag{5}$$

where $\boldsymbol{g} = (\delta \ln X, \delta \ln Z)$.

It is a straightforward matter to compute the kernels in equation (5). The linearized structure equations (2-4) formally can be written

$$\mathcal{B}\boldsymbol{f} = \boldsymbol{g}, \tag{6}$$

where $\mathcal{A}$ is a linear differential operator. The equation must be supplemented with appropriate boundary conditions which are derived from the requirement that conditions in the photosphere are unchanged, and which we adopt in the form $\ln\rho = 0$, $\ln L = 0$ at $r = R$. Substituting equation (6) into equation (5) yields

$$\frac{\delta\nu_i}{\nu_i} = \int_0^{\mathrm{R}} \boldsymbol{K}_{\boldsymbol{g}}^{(i)} \cdot \mathcal{B}\boldsymbol{f}\,\mathrm{d}r + \frac{F(\nu_i)}{E_l(\nu_i)} = \int_0^{\mathrm{R}} \mathcal{B}^*\boldsymbol{K}_{\boldsymbol{g}}^{(i)} \cdot \boldsymbol{f}\,\mathrm{d}r + \frac{F(\nu_i)}{E_l(\nu_i)}, \tag{7}$$

where $\mathcal{B}^*$ is the adjoint of $\mathcal{B}$. By demanding that the expressions on the right-sides of equations (1) and (7) be identical, we obtain

$$\mathcal{B}^*\boldsymbol{K}_{\boldsymbol{g}}^{(i)} = \boldsymbol{K}_{\boldsymbol{f}}^{(i)}. \tag{8}$$

Thus, the seismic kernels for the element abundances are obtained as solutions of the adjoint linearized structure equations. Structure function $\boldsymbol{g}$ may include variations of the microscopic properties such as opacity and nuclear reaction rates.

A selection of the kernels for two different pairs of the structure variables is shown in Fig.1.

2.2 Localized averages

The inversion procedure basically consists of constructing linear combinations of equations (1) or (5) for a set of observed modes, which provide localized averages of the structure parameters $\boldsymbol{f}$ and $\boldsymbol{g}$:

$$\overline{\boldsymbol{f}}(r_0) = \int_0^{\mathrm{R}} A_{\boldsymbol{f}}(r_0, r)\boldsymbol{f}\,\mathrm{d}r, \qquad \overline{\boldsymbol{g}}(r_0) = \int_0^{\mathrm{R}} A_{\boldsymbol{g}}(r_0, r)\boldsymbol{g}\,\mathrm{d}r. \tag{9}$$

We have applied the Backus-Gilbert optimally localized averaging technique [11]. To illustrate it consider the 'secondary' inversion for the abundances of hydrogen, $X(r)$, and heavy elements, $Z(r)$. In this case, $\boldsymbol{g} = (\delta \ln X, \delta \ln Z)$, and helioseismic equations (5) take the form:

$$\frac{\delta\nu_i}{\nu_i} = \int_0^R K^{(i)}_{X,Z}\;\delta\ln X\;\mathrm{d}r + \int_0^R K^{(i)}_{Z,X}\;\delta\ln Z\;\mathrm{d}r + \frac{F(\nu_i)}{E_l(\nu_i)}. \tag{10}$$

The Backus-Gilbert method is to construct appropriate linear combinations

$$\sum_i c_i(r_0)\frac{\delta\nu_i}{\nu_i} \tag{11}$$

of the data from coefficients $c_i(r_0)$ designed to make unimodular averaging kernels for one of the structure variables, say, X:

$$A_{X,Z}(r_0; r) = \sum_i c_i(r_0) K^{(i)}_{X,Z}(r) \tag{12}$$

well localized about a chosen location $r = r_0$ and the corresponding averaging kernels for the second variable, Z,

$$A_{Z,X}(r_0; r) = \sum_i c_i(r_0) K^{(i)}_{Z,X}(r) \tag{13}$$

small everywhere, subject to the data combination (11) being invariant under the transformation $\delta\nu_i/\nu_i \to \delta\nu_i/\nu_i - F(\nu_i)/E_l(\nu_i)$, where $F(\nu_i) = \sum_{\lambda=0}^{\Lambda} a_\lambda P_\lambda(\nu_i)$ for all constants a_λ, and where P_λ are polynomials. The localization of $A_{X,Z}$ is moderated by the requirement that the combination (11) is not excessively sensitive to errors σ_i in the data. This is achieved by minimizing, for chosen tradeoff parameters α and β, the quantity

$$\int_0^R \left[(A_{X,Z})^2(r - r_0)^2 + \beta(A_{Z,X})^2\right]\mathrm{d}r + \alpha\sum_i c_i^2\sigma_i^2, \tag{14}$$

subject to $\int_0^R A_{X,Z}dr = 1$ and the $\Lambda + 1$ additional constraints $\sum_i c_i P_\lambda(\nu_i)/E_l(\nu_i) = 0; \quad \lambda = 0, 1, 2, ..., \Lambda$.

The value of the regularization parameter α is chosen to balance the relative importance of obtaining a well localized average of $\delta \ln X$ with that of reducing the variance of the random errors, by choosing for instance, a point in the knee of the trade-off curve relating resolution and error magnification [11]. The other two parameters, β and Λ, control the susceptibility of the localized averages to contamination by the unknown structure function $\delta \ln Z$ and by

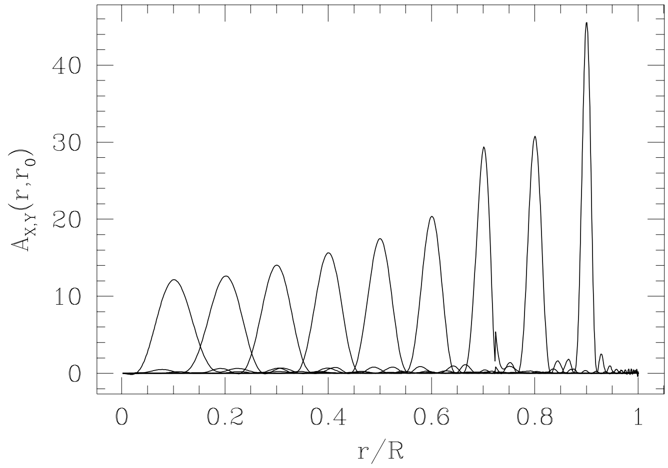

Figure 2: Localized averaging kernels for the hydrogen abundance, $A_{X,Z}$, which are linear combinations of the corresponding seismic kernels $K_{X,Z}$.

the surface uncertainties. With the proper values of α, β and Λ, the linear combination (11) represents essentially an average $\overline{\delta \ln X}$ of $\delta \ln X$, given by

$$\overline{\delta \ln X}(r_0) \equiv \int_0^R A_{X,Z}(r_0, r)\, \delta \ln X(r)\, \mathrm{d}r \approx \sum_i c_i \frac{\delta \nu_i}{\nu_i} \tag{15}$$

in the vicinity of $r = r_0$.

The spatial resolution of the averages can be characterized by a central coordinate and a resolution scale of the averaging kernels. These quantities usually represent some integral measure, 'center' and 'spread', of the kernels to account for their asymmetry and sidelobes.

A selection of the localized averaging kernels for the hydrogen abundance is shown in Fig.2. The averaging kernels were obtained as linear combinations of the seismic kernels, $K^{(i)}_{X,Y}$, of about 600 p modes of oscillations in the 5-min range. The typical radial resolution near the solar center is $0.05 - 0.07R$. The maximum of the averaging kernel closest to the center, that can be constructed for the p modes, is about at $0.05R$.

3 Inversion results

3.1 Data

The inverted data used in this analysis are combinations of 16 frequencies of low-degree modes ($l = 0$, 1 and 2) in the frequency range $2.5 \lesssim \nu \lesssim 3$ mHz taken from the IPHIR data set [12] and 598 frequencies of intermediate-degree modes (l = 4–140, ν = 1.5–3 mHz) observed at BBSO in 1988 [13].

3.2 Primary inversion

The results of the 'primary' inversion that is constrained only by the equations of hydrostatic support (2) are shown in Fig. 3. Fig.3a shows the relative difference of the ratio pressure to density (the isothermal sound speed, u) between the Sun and the reference solar model [2]. The

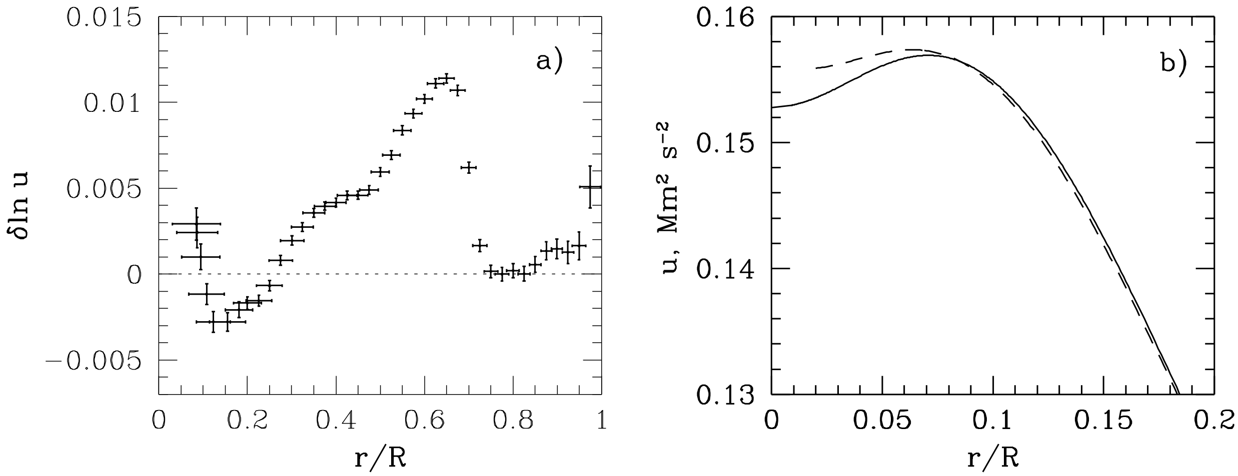

Figure 3: a) Optimally localized averages of the difference $\delta u/u$, where $u \equiv p/\rho$, between the Sun and the reference solar model, inferred from combinations of intermediate-degree mode frequencies from BBSO [13] and of the low-degree mode frequencies from IPHIR [12]. The horizontal bars represent the resolution lengths; the vertical bars represent standard errors. b) The structure function $u \equiv p/\rho$ of the reference model (solid curve) and of the Sun (dashed curve) inferred from the inversion shown in Fig. 3a.

difference is small in the adiabatically stratified convection zone occuping the outer 30% of the solar radius. The characteristic bump beneath the convection zone, between 0.3 and 0.7 R, is mainly a result of diffusion of helium [14], not taken into account in the reference model. The inversion shows a rapid variation of u in the core, the nature of which is unknown. However, such variation is typical for solar models with material mixing localized in the core. Fig.3b shows the inverted (dashed curve) and model (solid) profiles of u in the core. Depression near the center is as a result of the increased molecular weight, μ, caused by fusion hydrogen to helium.

Because the solar plasma is almost an ideal gas, $u \equiv p/\rho \approx \mathcal{R}T/\mu$. However, the temperature, T, and the molecular weight cannot be determined separately by helioseimology without additional constraints (Sec. 2.1).

3.3 Secondary inversion

We have carried out the secondary inversion for the helium abundance taking the same data set and the same reference solar model as for the primary inversion, and using the OPAL opacity and equation-of-state tables [15], and the nuclear reaction rates by Caughlan and Fowler [16].

The optimal averages inferred by inversion for the relative difference of X between the Sun and the model are shown in Fig.4a. Fig.4b shows the reconstructed (dashed curve) and model (solid curve) distributions of hydrogen in the Sun's interior. In the convective envelope, the mass fraction of hydrogen is significantly higher than in the model due to gravitational settling of helium and other heavy elements. We note that the estimate of the amount of helium in the convection zone depend entirely on the variation of the adiabatic exponent, γ, in the HeII ionization zone and are obtained using the equation of state. A version of the 'MHD' equation of state [17] gives the helium abundance $Y \approx 0.232 \pm 0.006$, whereas the OPAL equation of state

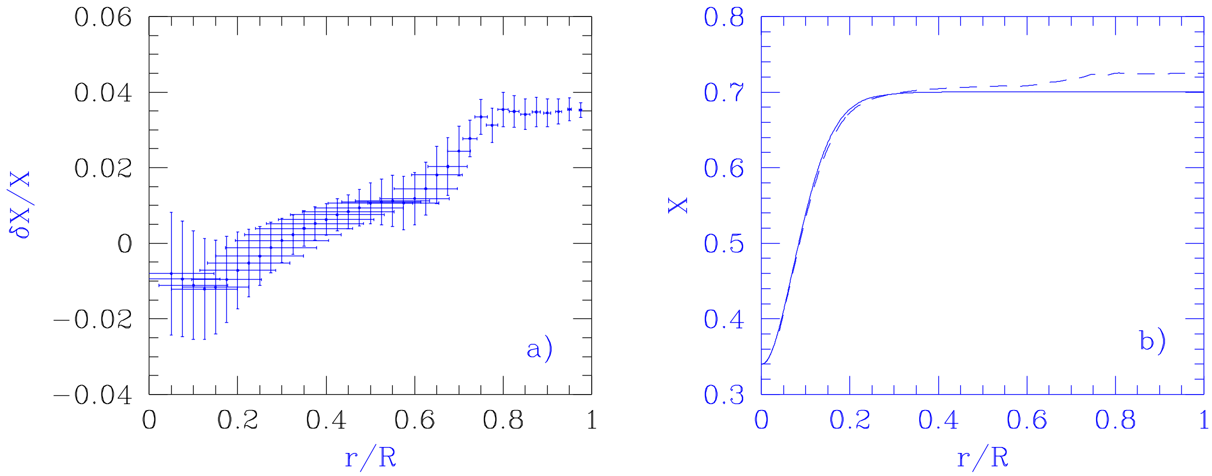

Figure 4: a) Optimally localized averages of the relative difference $\delta X/X$, where X is the abundance of hydrogen, between the Sun and the reference solar model, inferred from combinations of intermediate-degree mode frequencies from BBSO [13] and of the low-degree mode frequencies from IPHIR [12]. The horizontal bars represent the resolution lengths; the vertical bars represent standard errors. b) The hydrogen abundance of the reference model (solid curve) and of the Sun (dashed curve) inferred from the inversion shown in Fig. 4a.

[15] leads to $Y \approx 0.254 \pm 0.006$. The most recent version of the OPAL equation of state gives a slightly lower value: 0.248 ± 0.006. The difference between the MHD and OPAL equations of state has not been fully resolved. However, both estimates are substantially lower than the standard model value, $Y = 0.280$, and therefore, consistent with the general picture of the helium settling.

The variations of $\delta X/X$ in the radiative zone ($r/R < 0.7$) occur mainly because of helium diffusion towards the center. Diffusion is more efficient in the upper part of the convection zone ($0.6 < r/R < 0.7$) than in the deep interior. That explains the relatively steep variation of $\delta X/X$ in the layer just beneath the convection zone. The distribution of elements in this layer is also affected by rotationally induced mixing [18]. In the central core, there is, probably, 1% deficit of hydrogen. However, the error of the estimate is large (Fig. 4a).

3.4 Estimates of the solar core properties and the neutrino fluxes

High-energy neutrinos are generated at $r < 0.05R$ in the region which is not measured directly by p modes. The localized averages obtained by both the primary and the secondary inversion are centered outside this central region. Therefore, the inversion results have to be extrapolated to the center assuming smoothness of solar properties. Using the estimates of the structure function $u(r)$ and the abundances of hydrogen, $X(r)$, and heavy elements, $Z(r)$, one can deduce the solar temperature, $T(r)$, from the equation of state, and then compute the fluxes of solar neutrinos.

Here, we give only simple estimates of the fluxes using the approximate relations obtained by Gough [19]:

$$L_{\nu 1} \propto (1 + X_c), \quad L_{\nu 7} \propto (1 - X_c) X_c^{-1} T_c^7, \quad L_{\nu 8} \propto (1 - X_c)(1 + X_c)^{-1} T_c^{20.5}, \qquad (16)$$

where $L_{\nu 1}$, $L_{\nu 7}$ and $L_{\nu 8}$ are the fluxes of p-p, ^{7}Be and ^{8}B neutrinos, respectively; $T_{\rm c}$ and $X_{\rm c}$ are the central temperature and the hydrogen abundance.

From the inversions, we have:

$$\frac{\delta u_{\rm c}}{u_{\rm c}} \approx 0.01 \pm 0.002, \qquad \frac{\delta X_{\rm c}}{X_{\rm c}} \approx -0.01 \pm 0.015. \tag{17}$$

The equation of state of the ideal gas, $u \equiv p/\rho = \mathcal{R}T/\mu$, gives:

$$\frac{\delta T_{\rm c}}{T_{\rm c}} \approx \frac{\delta u_{\rm c}}{u_{\rm c}} + \frac{2}{5}\frac{\delta X_{\rm c}}{X_{\rm c}} \approx 0.006 \pm 0.008. \tag{18}$$

For the standard solar model, $T_{\rm c}^{\rm SSM} \approx 15.5 \times 10^6$K and $X_{\rm c}^{\rm SSM} \approx 0.340$, then, in the Sun, $T_{\rm c}^{\odot} \approx (15.70 \pm 0.13) \times 10^6$K, and $X_{\rm c}^{\odot} \approx 0.337 \pm 0.005$. Finally, from Eq. (16), obtain

$$L_{\nu 1}^{\odot} \approx (0.99 \pm 0.015) L_{\nu 1}^{\rm SSM}, \qquad L_{\nu 7}^{\odot} \approx (1.04 \pm 0.06) L_{\nu 7}^{\rm SSM}, \qquad L_{\nu 8}^{\odot} \approx (1.13 \pm 0.18) L_{\nu 8}^{\rm SSM}. \tag{19}$$

Therefore, the ^{7}Be and ^{8}B neutrino fluxes estimated from the helioseismic inversion are somewhat higher than the fluxes obtained from the standard solar model. Thus, the helioseismic results favor a MSW solution of the solar neutrino problem [20]. In addition, they may provide useful constraints on neutrino masses and mixing angles.

4 Conclusion

Helioseismology is a unique tool for determining the physical properties of the solar core. We have demonstrated how helioseismic inferences can be used for estimating the solar neutrino fluxes. The constraints on the properties of the core and on the neutrino fluxes obtained from the current helioseismic data are rather weak for two main reasons. First, the measurements of oscillation frequencies of low-degree p modes which probe the core are not sufficiently reliable at this time. The current data obtained by different groups have not yet provided a consistent picture of the core structure [21]. Also, because the data are inaccurate, the spatial resolution at the core is rather low and the errors of the estimated properties are large. To measure the frequencies accurately requires long continuous time series. Significant improvement in the integrity of the helioseismic data is expected from the ESA-NASA space mission SOHO [7]. The second reason for the uncertainty is that the temperature and the element abundances are the 'secondary' seismic parameters which can be estimated only through additional constraints such as the equation of state and the equation of thermal equilibrium. These constraints include microscopic properties (e.g. opacity, nuclear reaction rates) which are not known precisely. In principle, the uncertainties of the microscopic physics can also be tested seismologically.

As shown by J.Guzik [22] and S.Vauclair [18], helioseismology has provided important information about the solar structure, which has led to deeper understanding the physical processes in the star and to a significant improvement of its model. With more accurate frequency measurements, helioseismology will also provide reliable constraints on the hydrostatic and thermal stratification of the energy-generating core, that are essential for interpretation of the current and future solar neutrino experiments.

The author thanks Joyce Guzik, Douglas Morrison and Sylvie Vauclair for the useful discussions. The work was partly supported by a grant from NASA.

References

[1] Bahcall, J., 1995, *Nucl. Phys., Proc. Supp.*, **38**, 98.

[2] Christensen-Dalsgaard, J., Gough, D.O. & Thompson, M.J., 1991, *Astrophys. J.*, **378**, 413.

[3] Kosovichev A.G. & Fedorova A.V., 1991, *Sov. Astron.*, **35**, 507.

[4] Däppen, W., Gough, D. O., Kosovichev, A. G. and Thompson, M. J. 1991, in *Challenges to theories of the structure of moderate-mass stars* (ed. D.O.Gough and J.Toomre, Springer, Heidelberg), 111.

[5] Dziembowski, W.A., Pamyatnykh, A.A., Sienkiewicz, R., 1990, *Mon. Not. Roy. Aastr. Soc.*, **244**, 542

[6] Kosovichev, A.G., Christensen-Dalsgaard, J., Däppen, W., Dziembowski, W., Gough, D. & Thompson, M., 1992, *Mon. Not. Roy. Aastr. Soc.*, **259**, 536.

[7] *The SOHO Mission*, eds B.Fleck, V.Domingo & A.Poland, Dordrecht, Kluwer, 1995.

[8] Leibacher, J. these Proceedings

[9] Gough, D.O, Kosovichev, A.G., 1988, in *Seismology of the Sun and Sun-like Stars*, ESA SP-286, 195

[10] Gough, D.O. & Kosovichev, A.G., 1990, *Inside the Sun*, eds G.Berthomieu & M.Gribier, Dordrecht, Kluwer, 327.

[11] Backus, G. & Gilbert, F. 1968, *Geophys. J. R. astr. Soc.*, **16**, 169

[12] Toutain, T., C. Fröhlich, *Astron. & Astrophys.*, 1992, **257**, 287

[13] Libbrecht, K.G., Woodard, M.F., Kaufman, J.M., 1990, *Astrophys. J. Suppl*, **74**, 1129.

[14] Christensen-Dalsgaard, J., Proffitt, C.R., Thompson, M.J. 1993, *Astrophys. J. Lett*, **403**, L75.

[15] Rogers,F.J. & Iglesias, C.A.,1993, in *Seismic Investigation of the Sun & Stars.* ed.T.Brown, Ast.Soc.Pac., 155.

[16] Caughlan, G.R. & Fowler, W.A., 1988, *Atom. Nucl. Data Tabl.*, **40**, 283.

[17] Däppen, W., Mihalas, D., Hummer, D.G., Mihalas, B.W., 1988, *Astrophys. J.*, **332**, 261.

[18] Vauclair, S., these Proceedings.

[19] Gough, D.O., 1991, *Ann. N.Y. Acad. Sci.*, **647**, 199.

[20] Mikheev, S.P. & Smirnov, A., 1986, *Nuovo Cim*, **C9**, 17.

[21] Kosovichev, A.G., 1995, in *Helioseismology*, Fourth SOHO Workshop, ESA SP-376, 21.

[22] Guzik, J. these Proceedings.